

# The Extrema Edges

Pablo Andrés Arbeláez and Laurent D. Cohen

CEREMADE, UMR 7534 Université Paris Dauphine,  
Place du maréchal de Lattre de Tassigny,  
75775 Paris cedex 16, France  
`arbelaez@ceremade.dauphine.fr`, `cohen@ceremade.dauphine.fr`

**Abstract.** We present a new approach to model edges in the image. The method is divided in two parts: the localisation of possible edge points and their valuation. The first part is based on the theory of minimal paths, where the selection of an energy and a set of sources provides a partition of the domain. Then, the valuation is obtained by the creation of a contrast driven hierarchy of partitions. The method uses only the original image and supplies a set of closed contours that preserve semantically important characteristics of edges.

## 1 Introduction

The presence of sharp discontinuities in the image intensity seems to play a fundamental role for the interpretation of visual information in humans. Therefore, edge detection became soon a very active field of research in computer vision. Originally, edge detection techniques were motivated by the generalization to the plane of signal processing methods and the adaptation of regular analysis tools to the discrete domain. Thus, differentiation appeared as the natural operation to address the issue. Many discrete approximations of the gradient and models for the edges were proposed in the last decades. Examples include zero crossings of the laplacian [22], maxima in the gradient direction and crest lines of the gradient. In spite of their variety, a common element for many edge detection methods remained the use of local image information and a differential approach [30].

The classical approach to address this problem in the context of mathematical morphology is the characterisation of edges as the watershed lines of the gradient image [3]. Among the reasons for the large popularity of this method one can cite its intuitive definition, efficient algorithms for its implementation and the fact that the watersheds supply a set of closed contours. In the regular framework, the watersheds were defined as the skeleton by influence zones of a determined distance function [25]. These ideas established a bridge with PDE's based methods for computer vision and inspired a construction of the watersheds using curve evolution [21].

Our approach to the definition of edges in the image follows the opposite direction. The starting point is the theory of minimal paths, described in Section 2, where a partition of the domain is determined by the choice of an energy and

a set of sources. In Section 3, we study an energy called the linear variation, a generalization of the one dimensional total variation for functions of two variables. The application of this energy preserves the geometric structure of the function and allows to work on the original image. In Section 4, the choice of the image extrema as sources provides a piecewise constant simplification of the image, whose discontinuities are designated as the *extrema edges* of the image. Finally, in Section 5, we consider the valuation of the extrema edges using global image information. For this purpose, a family of nested partitions, guided by a notion of contrast, is constructed.

## 2 Minimal Paths and Energy Partitions

This introductory section presents the mathematical framework for the rest of the paper. Basic definitions are recalled and the notations settled.

Let  $\Omega \subset \mathbb{R}^2$  be a compact connected domain in the plane and  $x, y \in \Omega$  two points. A *path* from  $x$  to  $y$  designates an injective  $\mathcal{C}^1$  function  $\gamma : [0, L] \rightarrow \Omega$  such that  $\gamma(0) = x$  and  $\gamma(L) = y$ . Then, the image of  $\gamma$  is a rectifiable simple curve in the domain. The path is parameterized by the arclength parameter  $s$ , i.e:  $\|\dot{\gamma}(s)\| = 1, \forall s \in [0, L]$  and  $L$  represents the Euclidean length of the path. The set of paths from  $x$  to  $y$  is noted by  $\Gamma_{xy}$ .

**Definition 1.** *The surface of minimal action, or energy, of a potential function  $P : \Omega \times \mathcal{S}^1 \rightarrow \mathbb{R}^+$  with respect to a source point  $x_0 \in \Omega$ , evaluated at  $x$ , is defined as*

$$E_0(x) = \inf_{\gamma \in \Gamma_{x_0x}} \int_0^L P(\gamma(s), \dot{\gamma}(s)) ds .$$

When  $P$  depends only on the position  $\gamma(s)$  and is strictly positive almost everywhere, the computation of the energy can be performed using Sethian's *Fast Marching* method [28], as detailed in [6].

The surface of minimal action with respect to a set of sources  $S = \{x_i\}_{i \in J}$  is defined as the minimal individual energy:

$$E_S(x) = \inf_{i \in J} E_i(x) .$$

In the presence of multiple sources, a valuable information is provided by the interaction in the domain of a source  $x_i$  with the other elements of  $S$ , which is expressed through its *influence zone*:

$$Z_i = \{x \in \Omega \mid E_i(x) < E_j(x), \forall j \in J\} .$$

Thus, the influence zone is interpreted as the *shape* associated to  $x_i$ , determined the energy and the rest of the sources. The set of influence zones is noted by:

$$Z(E, S) = \bigcup_{i \in J} Z_i .$$

The *isoenergy set* is defined as the complementary of  $Z(E, S)$ :

$$I(E, S) = \{x \in \Omega \mid \exists i, j \in J, i \neq j : E_S(x) = E_i(x) = E_j(x)\} .$$

Therefore, the selection of an energy and a set of sources defines an *energy partition*  $\Pi(E, S)$  of the domain:

$$\Pi(E, S) = Z(E, S) \cup I(E, S) .$$

Energy minimizing paths have been used to address several problems in the field of computer vision, where the potential is generally defined as a function of the image. Examples include the global minimum for active contour models [6], shape from shading [17], continuous scale morphology [18], virtual endoscopy [8] and perceptual grouping [5].

### 3 The Linear Variation

In the usual approach for the application of minimal paths to image analysis, a large part of the problem consists in the design of a relevant potential for a specific situation and type of images. However, we adopt a different perspective and use the notions of the previous section for the study of a particular energy, whose definition depends only on geometric properties of the image.

#### 3.1 Energy Definition

For functions of one real variable, the variation is a functional with known properties [13], [27]. It was introduced by Jordan [16] as follows:

Let  $f : [0, L] \rightarrow \mathbb{R}$  be a function,  $\sigma = \{s_0, \dots, s_n\}$  a finite partition of  $[0, L]$  such that  $0 = s_0 < s_1 < \dots < s_n = L$  and  $\Phi$  the set of such partitions.

The *variation*, or *total variation*, of  $f$  is defined as

$$v(f) = \sup_{\sigma \in \Phi} \sum_{i=1}^n |f(s_i) - f(s_{i-1})| .$$

If  $f \in \mathcal{C}^1([0, L])$ , then the variation can be expressed as:

$$v(f) = \int_0^L |f'(s)| ds . \quad (1)$$

The linear variation is a generalization of the total variation for two variable functions:

**Definition 2.** *The linear variation of a function  $u : \Omega \subset \mathbb{R}^2 \rightarrow \mathbb{R}$  with respect to a source point  $x_0 \in \Omega$ , evaluated at  $x$ , is defined as*

$$V_0(u)(x) = \inf_{\gamma \in \Gamma_{x_0 x}} v(u \circ \gamma) .$$

Thus, the linear variation between two points is given by the minimal variation of the function on all the paths that join them.

**Definition 3.** *The space of functions of bounded linear variation of  $\Omega$ , noted by  $BLV(\Omega)$  is defined by*

$$BLV(\Omega) = \{u : \Omega \rightarrow \mathbb{R} \mid \forall x_0, x \in \Omega, \exists \hat{\gamma} \in \Gamma_{x_0 x} : V_0(u)(x) = v(u \circ \hat{\gamma}) < \infty\} .$$

In the sequel, we suppose that  $u$  has bounded linear variation.

If  $u$  is a continuously differentiable function, then (1) allows to reformulate  $V_0(u)$  as

$$V_0(u)(x) = \inf_{\gamma \in \Gamma_{x_0 x}} \int_0^L |D_{\hat{\gamma}} u(\gamma(s))| ds . \quad (2)$$

Thus,  $V_0(u)$  may be seen as a surface of minimal action for the potential  $P = |D_{\hat{\gamma}} u|$ , the absolute value of the directional derivative of  $u$  in the direction of the path.

The linear variation was introduced by Kronrod in a different formulation, as a part of a geometric theory for functions of two variables [19]. The intuitive notion expressed by this concept is illustrated in Fig. 1. Consider a particle moving along the graph of the function depicted on the left and starting at the source  $x_0$ . Then, as shown on the right, the value of  $V_0(u)$  evaluated at  $x$  represents the minimal sum of ascents and descents to be travelled to attain the point  $x$ .

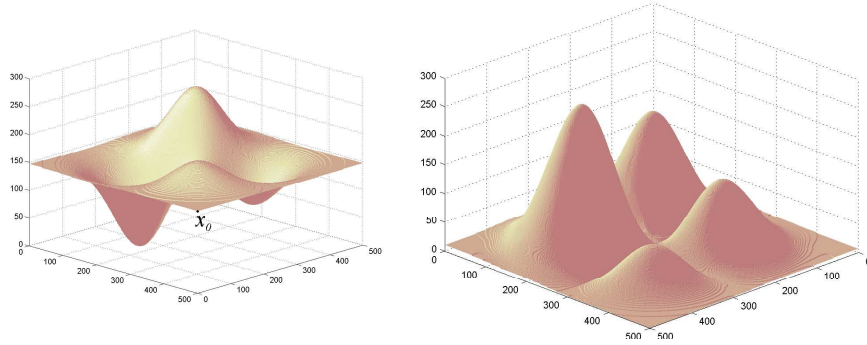


**Fig. 1.** Graphs of  $u$  and  $V_0(u)$ .

The *component* of  $u$  containing  $x$ , noted by  $K_x$ , is defined as the maximal connected subset of  $\Omega$  such that  $u(y) = u(x)$ ,  $\forall y \in K_x$ . The importance of this concept for the linear variation is given by the following proposition, whose proof is an immediate consequence of Def. 2.

**Proposition 1.** *The linear variation acts on the components of  $u$ :*

$$\forall x, y \in \Omega, K_x = K_y \Rightarrow \forall x_0, V_0(u)(x) = V_0(u)(y) .$$

Therefore, each component of  $V_0$  is a union of components of the function. Furthermore, for a set of sources  $S$ , each element of  $\Pi(V(u), S)$  is also a union of components of  $u$ . Thus, since the energy partitions induced by the linear variation preserve this geometrical structure of the function,  $V(u)$  presents a particular interest for image analysis.

### 3.2 Linear Variation and Image Distance

In the context of mathematical morphology, the energy associated to the potential  $P = \|\nabla u\|$ , given by the formula:

$$W_0(u)(x) = \inf_{\gamma \in \Gamma_{x_0 x}} \int_0^L \|\nabla u(\gamma(s))\| ds$$

has been used to define the watershed transform in a continuous domain [25], [23]. If, as for the class of Morse functions,  $u$  has only isolated critical points, then  $W_0$  induces a distance transform on  $\Omega$ , called the *image distance* [25] or the *topographic distance* [23].

The relation between  $W$  and  $V$  in the regular framework is expressed by the following property:

**Proposition 2.** *If  $u$  is a Morse image,  $u \in BLV(\Omega)$  and  $x_0 \in \Omega$ , then*

$$|u(x) - u(x_0)| \leq V_0(u)(x) \leq W_0(u)(x), \forall x \in \Omega .$$

*In particular, if  $x$  and  $x_0$  belong to a line of steepest slope for  $u$ , then*

$$|u(x) - u(x_0)| = V_0(u)(x) = W_0(u)(x) ,$$

The proof of this proposition [1] follows from simple calculus and the fact that  $|D_{\dot{\gamma}}(u)| = \|\nabla u\|$  when  $\dot{\gamma}$  is parallel to the gradient, by definition .

The behaviour of these two energies can be compared using the test image on the right column of Fig. 2. In this case,  $S = \{x_0, x_1\}$ , where  $x_0$  is the upper left and  $x_1$  the lower right corners of the domain; the function is given by the formula  $u(x) = c\|x - x_0\|$ . The central column shows the effect of the linear variation: as a consequence of Prop. 1,  $u$  and  $V_S(u)$  have in this example the same components and only their level is modified. The isoenergy set  $I(V(u), S)$ , shown on black, is the component whose level is the average of the sources' levels. On the right column it can be observed that, since  $\|\nabla u\|$  is constant,  $W_S(u)$  is proportional to the Euclidean distance to the closest source and  $I(W(u), S)$  corresponds to

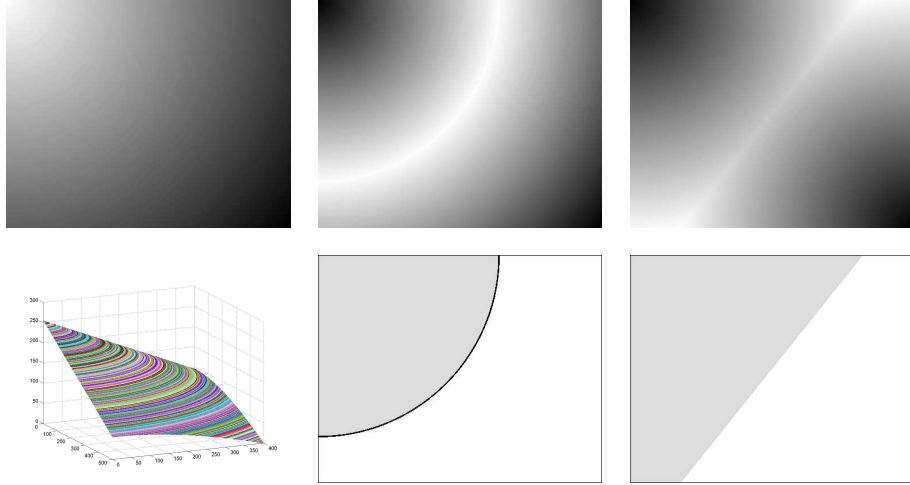


**Fig. 2.** From left to right. Top:  $u$ ,  $V_S(u)$  and  $W_S(u)$ . Bottom: Graph of  $u$ , energy partitions  $\Pi(V(u), S)$  and  $\Pi(W(u), S)$

the medial line between the sources; however, because of the quantification, the isoenergy set is absent from the partition. Note that any other function for which  $\|\nabla u\|$  is constant would produce the same partition  $\Pi(W(u), S)$ . This example illustrates how  $\Pi(V(u), S)$ , the partition induced by  $V$ , preserves the image information better than  $\Pi(W(u), S)$ .

### 3.3 Discrete Domain

Consider now that the image  $u$  has been sampled on a uniform grid. As pointed out in Sect. 1, the image distance  $W$  can be implemented using the Fast Marching method, with complexity  $O(M \log(M))$ , where  $M$  is the total number of sampling points. However, since the potential of the linear variation in (2) depends not only on the position but also on the path direction, this approach cannot be used for its construction.

Nevertheless, the election of a digital connectivity defines an adjacency graph  $G$ , where the nodes correspond to discrete components and the links join neighbouring components. Since  $V$  acts on the components of the function, we propose to construct the discrete linear variation directly on  $G$ .

A path on  $G$  joining the components of two points  $p$  and  $q$  is a set  $\gamma = \{K_0, \dots, K_n\}$  such that  $K_p = K_0$ ,  $K_n = K_q$ ,  $K_i$  and  $K_{i-1}$  are neighbours,  $\forall i = 1, \dots, n$ .  $\Gamma_{pq}^G$  denotes the set of such paths. Each element of  $\Gamma_{pq}^G$  corresponds then to a class of discrete paths between  $p$  and  $q$ .

Thus, the expression of the discrete linear variation of  $u$  at a point  $q$  with respect to the source  $p$  becomes

$$V_p(u)(q) = \min_{\gamma \in \Gamma_{pq}^G} \sum_{i=1}^n |u(p_i) - u(p_{i-1})| ,$$

where  $p_i \in K_i, \forall i = 1, \dots, n$ .

Hence, the calculation of  $V_p(u)$  is reduced to finding the path of minimal cost on a graph. This classical problem can be solved using, for instance, Dijkstra's greedy algorithm [9], [20]. The complexity of this implementation for the linear variation is then  $O(N \log(N))$ , where  $N$  is the total number of discrete components of the image. Furthermore, if  $u$  takes integer values, the sorting step in the update of the narrow band can be suppressed and the complexity is reduced to  $O(N)$ .

## 4 The Extrema Edges

### 4.1 The Extrema Partition

Surfaces of minimal action are often appropriated for a local level of analysis in the image. This is due to the fact that Def. 1 is based on an integration along the paths. As a consequence of the oscillatory nature of images, the energies of this type tend to lose their meaning when the shapes become too large. Besides, replacing a source  $x_i \in S$  by another point  $\hat{x}_i \in Z_i$  usually modifies the energy partition.

Therefore, the set of sources must be selected with care. Firstly, they should be physically representative of the image content. Secondly, each significant feature should contain at least one of them. Since they satisfy these conditions, the image extrema appear as natural candidates for the sources.

**Definition 4.** *The extrema partition (EP) of an image  $u : \Omega \rightarrow \mathbf{R}$  is defined as  $\Pi(V(u), ext(u))$ , the energy partition induced by the linear variation and the set of extremal components of  $u$ .*

Thus, Prop. 1 implies that the elements of the EP are unions of components of  $u$  and they can be divided in two types. On the one hand, the influence zones of the extrema, interpreted as the *atoms* or *elemental shapes* of the image. On the other hand, the elements of the isoenergy set  $I(V(u), ext(u))$  are designated as *boundary components* of the atoms.

Figure 3 illustrates our approach on a simple regular case. The function  $u$ , on the left, is a gaussian blob, where the only extremal components are the centre and the border of the squared domain. The image on the middle shows the energy  $V_{ext(u)}(u)$ , rescaled by a factor of 2 for better visualization. On the right, the extrema partition  $\Pi(V(u), ext(u))$  is composed by two elemental shapes and a circular boundary component, fragmented by the quantization.

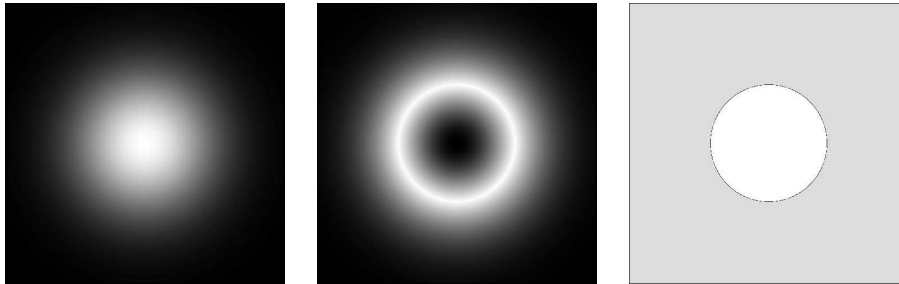


**Fig. 3.** From left to right: test image, energy end extrema partition.

#### 4.2 Definition of the Extrema Edges

The effects of the extrema partition on smooth functions, suggest the use of the boundary components to model edges. Nevertheless, as shown on the previous examples, the quantification of levels and the subsampling often result in the loss of important parts of the isoenergy set. An alternative to surround this problem is to consider an energy partition composed only by shapes. Consequently, the elements of the isoenergy set are assigned to one of their neighbouring influence zones. Then, a *shape model*, determined by the distribution of the image values on the shape, can be chosen to represent each influence zone. The simplest models are constant; examples are the mean or median value on the influence zone and the value of the image at the source. Therefore, the valuation of each shape in the energy partition by its model produces a piecewise constant approximation of the image, designated as a *mosaic image*. The mosaic corresponding to the extrema partition will be called the *extrema mosaic (EM)* of  $u$ . Generally, the intensity at the extremum represents accurately the atom's levels. In the sequel, unless stated differently, this election was adopted.

**Definition 5.** *The Extrema Edges of an image  $u$  are defined as the discontinuities of its extrema mosaic  $EM(u)$ .*

Note that, since the extrema edges are defined as the boundaries of the atoms, they provide a set of closed contours. Figure 4 shows, on the left, a real image and, on the right, its extrema mosaic. In this example, the number of components in the simplified image is reduced by a factor of 68. Nevertheless, note how the extrema edges model accurately the contour information and, particularly, semantically important characteristics of edges such as corners and junctions. Furthermore, the method seems to perceptually improve the image. This impression is due to the fact that, since components belonging to blurred contours and transition zones are generally not extremal, they are absorbed by a neighbouring atom. Consequently, the blur of the original image is reduced. Besides, the choice of the image value at the extremum as the atom model enhances the contrast in the extrema mosaic.





Fig. 4. Image and extrema mosaic

### 4.3 Extrema Edges and Watersheds

In mathematical morphology, the edges in an image  $u$  are usually modelled as the watershed lines of the modulus of its gradient,  $g = \|\nabla u\|$  [3], [26]. Their construction can then be obtained by a *flooding* [2]: the image, seen as a topographical surface, is pierced at its regional minima and progressively immersed in water. The water floods uniformly the valleys, or catchment basins of the minima, and, at the points where two lakes meet, a dam is built. When the surface is totally immersed, the union of the dams forms the watershed lines. This formulation of the watershed transform allowed efficient algorithms for its implementation [29] and allowed the formalization of the watersheds in the continuous domain as the skeleton by influence zones of the image distance [25]. Last, but not least, it suggests the interpretation of the minima of  $g$  as the dual concept of edges: the sources. In our notation, starting at a source  $x_0 \in \Omega$ , this energy can be written as

$$\widehat{W}_0(g) = W_0(g) + g(x_0) . \quad (3)$$

Thus, the energy associated to the segmentation by watersheds of an image  $u$  can be expressed as

$$\widehat{W}_{min(g)}(g) = \inf_{m_i \in min(g)} \widehat{W}_i(g) ,$$

where  $min(g)$  denotes the set of regional minima of  $g$ . This continuous formulation inspired the implementation of the watersheds using the Fast Marching method [21].

Therefore,  $\Pi(\widehat{W}(g), min(g))$ , the energy partition associated to the watershed transform, has the following interpretation: the isoenergy set  $I(\widehat{W}(g), min(g))$

corresponds to the watershed lines of  $g$  and represent the edges in  $u$ . Besides,  $Z(\widehat{W}(g), \min(g))$ , the shapes of the minima, coincide with the lakes, or catchment basins of the topographical surface.

If we use  $V$  instead of  $W$  in (3), we obtain the following result, whose proof [1] is based on Prop. 1 and 2 and the fact that, for Morse images, each catchment basin corresponds to the set of lines of steepest slope ending at its minimum [25].

**Proposition 3.** *If  $g$  is a Morse image and  $g \in BLV(\Omega)$ , then*

$$I(\widehat{V}(g), \min(g)) = \bigcup_{x \in I(\widehat{W}(g), \min(g))} K_x$$

Thus, the isoenergy set of  $\widehat{V}$  coincides with the set of components of the watershed lines. Hence, in the continuous domain, the use of  $V$  on the gradient generally produces edges thicker than the watersheds.

In practice, as happens for the boundary components, the watersheds are usually fragmented in real images. Therefore, in order to compare the extrema edges and the watersheds, we use their corresponding mosaics. Indeed, the construction of both mosaics depends on the same factors: the digital connectivity, the gray level on the shapes and the rule of assignation for the isoenergy set. However, the fundamental difference is that the former is defined in the original image, while the latter is built on the modulus of its gradient. Consequently, the watershed lines depend also on the choice of a discrete approximation of the gradient. Moreover, gradient operators are sensitive to noise and usually smooth the image to well pose differentiation. Since the smoothing step implies a loss of information in the image content, the watersheds suffer from limited resolution in certain cases. These problems cannot be neglected in fields where the precision of the extracted features is an essential issue, as in medical image analysis.

Figure 5 depicts the mosaics associated to the different models of edges presented. The first row shows the original image, a detail of the *cameraman*, and the extrema mosaic. The second row depicts, on the left, the watershed mosaic constructed on the morphological gradient and, on the right, the mosaic corresponding to the choice of  $\widehat{V}$  as the energy and the gradient's minima as sources. For all the cases 8-connectivity was used, the shape model was the source's level and the points in the isoenergy set were assigned to the first source to attain them. As a consequence of the spatial distribution of the sources and their large number, all the methods preserve the principal features in the scene, such as the silhouette of the man. However, the extrema mosaic enhances perceptually important details such as the mouth or the inner parts of the camera that are lost in the mosaics of the second row. The loss of information is due to the absence of regional minima inside those features and, even if the result may be improved by changing the type of gradient operator or the connectivity, the problem is intrinsic to the use of the gradient image. Finally, since Prop. 3 implies that the partitions  $\Pi(\widehat{W}(g), \min(g))$  and  $\Pi(\widehat{V}(g), \min(g))$  differ mainly in their isoenergy set, the two mosaics in the second row are almost identical.



**Fig. 5.** Above: original image and extrema mosaic. Below: mosaics of the energy partitions  $\Pi(\widehat{W}(g), \min(g))$  and  $\Pi(\widehat{V}(g), \min(g))$ .

## 5 Valuation of the Extrema Edges

Once a set of candidates for the edge points has been defined, the next problem is their valuation. In this section, we propose to construct a contrast driven hierarchy of partitions to provide global image information for the valuation of the extrema edges.

The idea of progressively merging regions of an initial partition has been used for a long time to address image segmentation problems [4], [15], [7], [12]. An efficient implementation of this idea can be obtained with a graph based region merging process, as described in [14] and [10]. This type of algorithms works on a *Region Adjacency Graph* (RAG), where the nodes correspond to connected regions of the domain and each region is represented by a model; the links encode the vicinity relation between regions and are weighted by a dissimilarity measure. The dissimilarity  $\mathcal{D}$  is a function defined for every couple of neighbouring regions and takes values in an interval  $I = [0, A]$ , referred as the set of *indices* or *scales*.

The initial partition, the dissimilarity and the region model determine an order of merging; the strategy consists on removing the links in the RAG for increasing values of the dissimilarity and merging the corresponding regions.

For any threshold  $\lambda \in I$ , the nodes remaining in the RAG represent a partition  $\Pi_\lambda$  of the domain. Performing the merging until a single region remains produces a family of nested partitions, or hierarchy,  $\{\Pi_\lambda\}_{\lambda \in I}$  where every region in  $\Pi_\mu$  is a disjoint union of regions in  $\Pi_\lambda$ , for  $\mu \geq \lambda$ .

The watershed flooding of a gradient image provides a classical example of hierarchical segmentation: the topographical surface is again flooded from its minima but, instead of building a dam at the meeting points, the lakes merge. Increasing levels of water produce coarser partitions and the resulting hierarchy is known as the *dynamics* [11]. In terms of a region merging process, the initial partition is composed by the watershed mosaic and the dissimilarity is defined as the height of the saddle point between two adjacent lakes, *i.e.* the minimal value of the gradient in the common border of the regions [24].

An advantage of using a hierarchy of partitions is that the location of contours is preserved through the scales. Additionally, when the dissimilarity expresses a notion of contrast, the concept of *saliency* of a pixel, defined as the highest index  $\lambda$  for which the pixel belongs to a contour of  $\Pi_\lambda$ , acquires a particular interest. The *contour map*, obtained by the valuation of each pixel by its saliency, is more than a simple edge map: it provides a compact description of the hierarchy in a single image. A threshold  $\lambda$  in this image supplies the set of closed contours of the corresponding partition  $\Pi_\lambda$ . The saliency was used in [26] to valueate the watershed lines with the hierarchy of dynamics.

In order to strongly relate the process to the information provided by the extrema mosaic and to make the merging order independent of the region model, we measured the dissimilarity on the initial partition. Moreover, since the purpose of the resulting hierarchy is to valueate the extrema edges, the dissimilarity was defined using boundary information. A typical choice for the dissimilarity is the average levels' difference in the common border of the regions, noted by  $\mathcal{D}_a$ .

Figure 6 exemplifies the approach on the *cameraman* test image. The first row shows the extrema mosaic and the contour map for  $\mathcal{D}_a$  in 8-connectivity, where a low intensity represents a high saliency. The second row depicts, on the left, the partition for a dissimilarity of  $\lambda = 54$ , with average grey level as the region model. On the right, the corresponding threshold in the contour map is shown. Note how the chosen dissimilarity expresses a notion of contrast between adjacent regions; at the scale presented, only contrasted regions remain, regardless of their size.

As a last example, Fig. 7 illustrates the accuracy of our approach for an application in medical image analysis. The goal was to detect a disease called the *drusen* - the white spots - in images of the eye fundus, as the one shown on the top left. The variations in the background's intensity in retinal angiographies as well as the absence of abrupt discontinuities in the drusen boundaries make their extraction a difficult problem with classical edge detection methods. The top right image shows the contour map of the original image. The image was

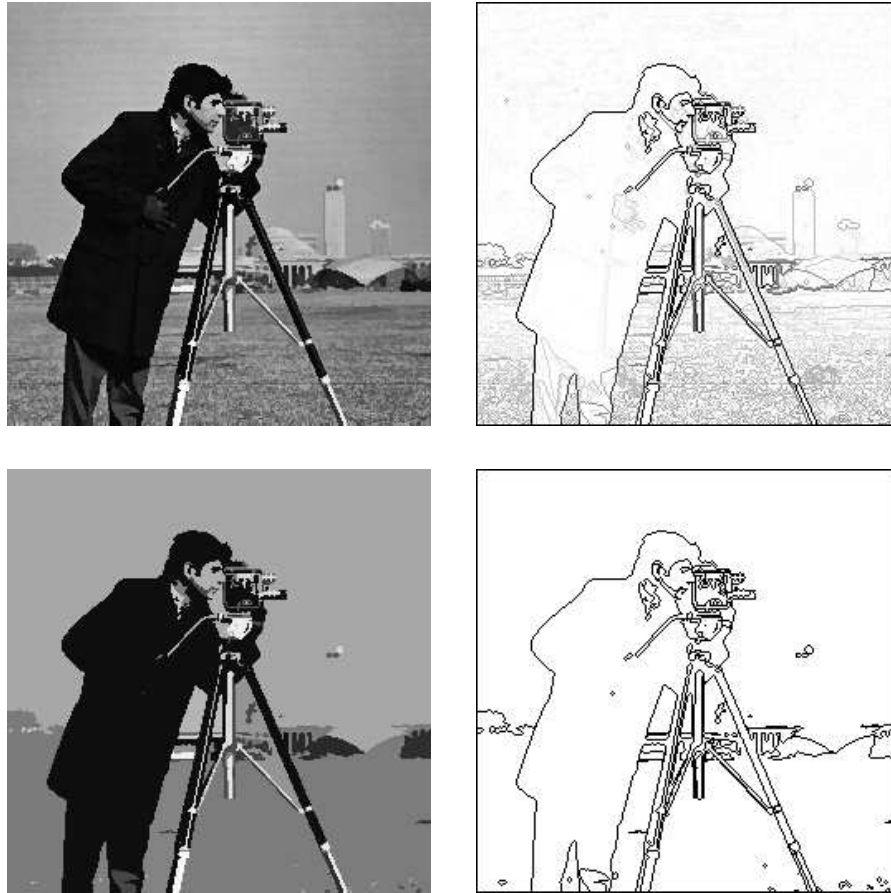


**Fig. 6.** Row 1: Extrema mosaic and contour map. Row 2: Segmentation for  $\lambda = 54$  and corresponding threshold in contour map

rescaled for better visualization, but the scale  $\lambda$  at which a single region remains is only 6. Since the transitions in the image are smooth, the resulting contours are blurred. In contrast, the second row depicts the application of our method. On the left, we can observe the extrema mosaic, where the drusen can be clearly distinguished from the background. The right image depicts the contour map of the EM, where  $\lambda = 58$ . It can be observed how the method provides the location and shape of the drusen with precision. Furthermore, their saliency can be used to measure the magnitude of the disease. In future work, we intend to use our approach to track the evolution of drusen on time.

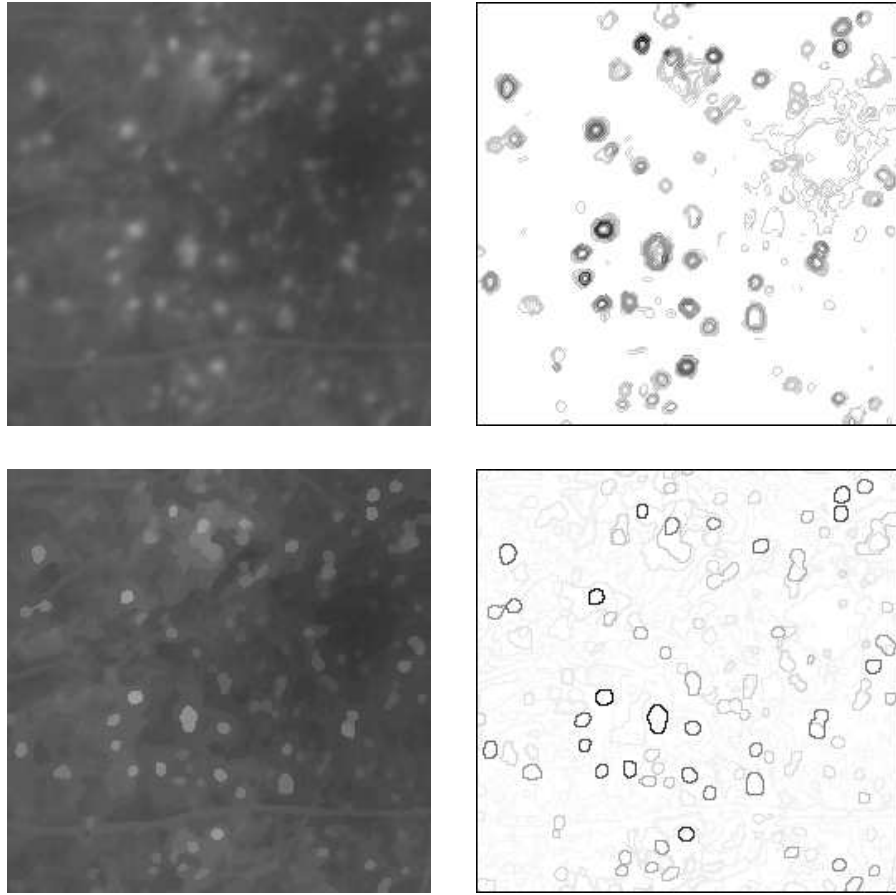


**Fig. 7.** Row 1: original image and contour map. Row 2: extrema mosaic and contour map.

## 6 Conclusion and Perspectives

We presented a new approach to model edges in the image. The method is divided in two parts. First, a set of possible edge points, the extrema edges, is defined and then a measure of saliency is assigned to every point in this set. The extrema edges are defined as the discontinuities of the mosaic image associated to the energy partition  $\Pi(V(u), ext(u))$ . Their valuation is obtained using global information through a family of nested partitions guided by a notion of contrast. The method provides a set of closed contours that preserve semantically important characteristics of edges.

Finally, this paper focused on monochrome images in order to empathize the mathematical formulation and properties of the extrema partition. However,

the results presented can be applied to color images directly by considering the brightness component. The generalization of our approach to color images will be the subject of our next report.

## References

1. Author, *Application of the Linear Variation to Image Analysis*, Technical Report, 2003.
2. S. Beucher, *Segmentation d'images et morphologie mathématique*. PhD Thesis, École des Mines de Paris, 1990.
3. S. Beucher and F. Meyer *The Morphological Approach to Segmentation: The Watershed Transformation*. In *Mathematical Morphology in Image Processing*, pp. 433-481, E.R. Dougherty, Ed. M. Dekker, New York, 1992.
4. C. R. Brice and C. L. Fenema *Scene Analysis using Regions*. *Artificial Intelligence*, 1: 205-226, 1970.
5. L. D. Cohen *Multiple contour finding and perceptual grouping using minimal paths*. In *Journal of Mathematical Imaging and Vision*, Vol. 14, No. 3, pp. 225-236, 2001.
6. L. D. Cohen and R. Kimmel, *Global minimum for active contour models: A minimal path approach*, *International Journal of Computer Vision*, Vol. 24, No. 1, pp. 57-78, 1997.
7. L. D. Cohen, L. Vinet, P. Sander and A. Gagalowicz, *Hierarchical Region Based Stereo Matching*. In *Proc. CVPR'89*, pp. 416-421, San Diego, California, 1989.
8. T. Deschamps and L. D. Cohen, *Fast extraction of minimal paths in 3D images and applications to virtual endoscopy*. In *Medical Image Analysis*, Vol. 5, No. 4, pp. 281-299, 2001.
9. E.W. Dijkstra *A Note on two problems in connection with graphs*. *Numerische Mathematic*, Vol. 1, pp.269-271, 1959.
10. L. Garrido, P. Salembier and D. Garcia, *Extensive operators in partition lattices for image sequence analysis*. In *Signal Processing: Special issue on Video Sequence Segmentation*, 66(2):157-180, April 1998.
11. M. Grimaud, *New Measure of Contrast: Dynamics*. *Image Algebra and Morphological Processing III*, San Diego, CA. *Proc. SPIE*, 1992.
12. R. Haralick and L. Shapiro *Computer and Robot Vision*. Vol. I, Adison Wesley, 1992.
13. E. Hewitt and K. Stromberg *Real and Abstract Analysis*. Springer Verlag, 1969.
14. R. Horaud and O. Monga *Vision par Ordinateur*. Hermes, Paris, 1995.
15. S. L. Horowitz and T. Pavlidis *Picture segmentation by a directed split and merge procedure*. *Second Int. joint Conf. on Pattern Recognition*, pp.424-433,1974.
16. C. Jordan *Sur la Série de Fourier*. *C. R. Acad. Sci. Paris Sér. I Math.* **92**, No. 5, (1881), pp.228-230.
17. R. Kimmel and A.M. Bruckstein, *Global Shape from Shading*. *CVIU*, Vol. 62, No. 3, pp 360-369, 1995.
18. R. Kimmel, N. Kiryati and A. M. Bruckstein. *Distance maps and weighted distance transforms*. *Journal of Mathematical Imaging and Vision*, Special Issue on Topology and Geometry in Computer Vision, 6:223-233, 1996.
19. A. S. Kronrod, *On functions of two variables*. *Uspehi Mathematical Sciences.* **5** (35), 1950.
20. R. Kruse and A. Ryba, *Data structures and program design in C++*. Prentice Hall, New York, 1999.

21. P. Maragos and M. A. Butt *Curve Evolution, Differential Morphology and Distance Transforms Applied to Multiscale and Eikonal Problems*. Fundamenta Informaticae 41, pp. 91-129, IOS Press, 2000.
22. D. Marr and E. Hildreth, *Theory of Edge Detection*. Proc. of Royal Society of London **B-207**, pp.187-217, 1980.
23. F. Meyer, *Topographic distances and watershed lines*. In Signal Processing 38, pp. 113-125, Elsevier 1994.
24. F. Meyer, *Hierarchies of Partitions and Morphological Segmentation*. In Scale Space and Morphology in Computer Vision, Michael Kerckhove Ed., Proc. Scale-Space 01, pp. 161-182, Vancouver, Canada 2001.
25. L. Najman, *Morphologie Mathématique: de la Segmentation d'Images à l'Analyse Multivoque*. PhD Thesis, Université Paris Dauphine, 1994.
26. L. Najman and M. Schmitt, *Geodesic Saliency of Watershed Contours and Hierarchical Segmentation*. In IEEE Transactions on Pattern Analysis and Machine Intelligence, Vol. 18, No. 12, December 1996.
27. I.P. Natansson, *Theory of Functions of a Real Variable*. Frederick Ungar Publishing Co., New York, 1964.
28. J.A. Sethian, *Level Set Methods and Fast Marching Methods*. Cambridge Univ. Press, Cambridge, UK,1999.
29. L. Vincent and P. Soille, *Watersheds in Digital Spaces: an Efficient Algorithm Based on Immersion Simulations*, IEEE Trans. Patt. Anal. Mach. Intell., 13, 6, pp.583-598, 1990.
30. D. Ziou and S. Tabbone, *Edge Detection Techniques- An Overview*, Technical Report, No. 195, Dept. Math. and Informatics. Universite de Sherbrooke, 1997.